

Bilayer growth of nanoscale Co islands on Cu(111)

N. N. Negulyaev,¹ V. S. Stepanyuk,² P. Bruno,² L. Diekhöner,^{3,4} P. Wahl,⁴ and K. Kern⁴

¹*Fachbereich Physik, Martin-Luther-Universität, Halle-Wittenberg, Friedemann-Bach-Platz 6, D-06099 Halle, Germany*

²*Max-Planck-Institut für Mikrostrukturphysik, Weinberg 2, D-06120 Halle, Germany*

³*Institut for Fysik og Nanoteknologi, Aalborg Universitet, Skjernvej 4, DK-9220 Aalborg, Denmark*

⁴*Max-Planck-Institut für Festkörperforschung, Heisenbergstrasse 1, D-70569 Stuttgart, Germany*

(Received 4 October 2007; revised manuscript received 20 December 2007; published 28 March 2008)

Combining kinetic Monte Carlo and molecular static simulations, we follow at the atomic scale the growth of Co nanoislands on Cu(111) surface over a wide range of surface temperatures (130–300 K). Atomistic processes responsible for the interlayer mass transport of Co atoms and the formation of 2 ML high nanoislands at temperatures >200 K are revealed. Transition from the two- to the three-dimensional growth mode with decreasing the temperature is demonstrated. Strain relaxations induced in the Cu substrate and in the Co nanoislands are found to have a strong impact on the formation of triangle Co islands at room temperatures. Results of our theoretical studies are supported by the scanning tunneling microscope measurements.

DOI: [10.1103/PhysRevB.77.125437](https://doi.org/10.1103/PhysRevB.77.125437)

PACS number(s): 61.46.–w

I. INTRODUCTION

Fundamental properties such as chemical reactivity or magnetism of thin metal films and nanostructures depend on their detailed structure and the substrate on which they are grown. Epitaxial growth of metal on metal single crystal surfaces has therefore been extensively studied. An atomistic description has experimentally become possible using the scanning tunneling microscope (STM) and theoretically using kinetic Monte Carlo (kMC) simulations based on calculations of activation barriers for atomic diffusion. Depending on the detailed energetics of the surface/adsorbate system and the kinetics of the reaction pathways involved, the growth normally follows one of three characteristic modes: layer by layer growth (Frank–van der Merwe), island growth (Volmer–Weber), or island growth on top of a wetting layer (Stranski–Krastanov).¹ The morphology of the grown structures depends on the flux of incident atoms and the diffusivity on the surface, which is interlinked to the intrinsic energetics of the system and the surface temperature.

Here, we concentrate on the growth of Co on Cu(111) surface in the low coverage regime. Cobalt thin films on Cu(111) are model systems for magnetic investigations. Therefore, recently, they were widely studied structurally^{2–5} and electronically.^{6–10} It is well known that Co on Cu(111) grows epitaxially, initially following the fcc stacking of the Cu substrate.^{3,4} Co forms dendritic shaped islands at low temperatures and compact triangular shaped islands at room temperature (RT).^{2,5} The triangular islands are always 2 ML high at low doses. This peculiar growth has also been observed for other related systems, for instance, Co on Ag(111) (Ref. 11) and Co on Pd(111).¹² Later, after forming these 2 ML high islands, the third and subsequent layers grow on top in a three-dimensional growth mode as in the Volmer–Weber picture. Interesting studies on atomistic processes during growth of Co on Cu(111) have been performed by Prieto *et al.* by means of STM.¹³ Diffusion barriers of atomic processes have been estimated by analyzing STM data in terms of simple phenomenological models.

The goal of our work is to understand the epitaxial growth of Co islands on Cu(111) surface at the atomic scale. We

perform kMC simulations with energy barriers of all relevant events calculated by means of the molecular static (MS) method with *ab initio* based interatomic potentials. We reveal that the formation of bilayer high nanoislands at RT can be explained qualitatively from the energy barriers of the interlayer mass transport. The triangular shape of Co islands at RT is found to be due to anisotropic corner diffusion. The detailed kMC simulations reveal how the overall shape of the Co nanoislands evolves and we find a perfect agreement with experimental STM data in the temperature range from 130 to 300 K.

The paper has the following structure. In Sec. II, we describe the experimental setup and the MS-kMC model used for our simulations. In Sec. III, we present the results of theoretical and experimental studies of epitaxial growth of Co nanoislands on Cu(111) in submonolayer regime. Section III is divided into three parts. In Sec. III A, we concentrate on the main atomistic processes, responsible for the growth of triangular bilayer Co islands at RT. In Sec. III B, we present the results of the kMC simulations at different temperatures and compare them with the STM measurements. In Sec. III C, we demonstrate the role of strain relaxations induced in the Cu substrate and Co nanostructures during self-organization of Co nanoislands.

II. COMPUTATIONAL METHODS AND EXPERIMENT

For the simulation of growth of Co on Cu(111), we apply the three-dimensional kMC model using diffusion barriers for many atomic events calculated by means of the MS method. The kMC model describes the elementary stochastic processes (deposition, atomic diffusion, and interlayer mass transport) in terms of reaction rates to avoid explicit calculation of unsuccessful attempts. This model was developed by Fichthorn and Weinberg¹⁴ and was used in several recent studies.^{15,16} The rate ν of an atomic process is calculated using the Arrhenius expression $\nu = \nu_0 \exp(-E_D/k_B T)$, where ν_0 is the prefactor, T is the temperature, and E_D is the activation barrier. In the framework of this model, the activation barrier for diffusion of atom depends on (i) N_i , the number of

neighboring atoms in the initial configuration, (ii) N_f , the number of neighboring atoms in the final configuration, and (iii) L , the number of the layer, where an atom is located [i.e., $E_D = E_D(N_i, N_f, L)$]. Prefactors for all events are set to 10^{12} Hz, while for a monomer diffusion [migration of a single Co adatom on a clean Cu(111) surface], we use 10^9 Hz. The exploiting of smaller prefactor for the monomer diffusion induces a higher island density which is necessary to reduce the computational demands (the similar procedure has been proposed in the recent study of Ovesson *et al.*¹⁵). However, results of the growth process of nanoislands (their shape and height) do not depend on this choice as it has been tested by employing other prefactors for monomer diffusion (we have tried the following values of prefactors: 10^{10} and 10^8 Hz). The kMC simulations are carried out on a close-packed (111) lattice consisting of 392×452 atoms (100×100 nm²), and periodic boundary conditions are applied along the surface plane. Both fcc and hcp sites are involved in our simulations. Co atoms are deposited on the substrate randomly. The deposition flux F is set to 0.001 ML/s, which is close to the experimental conditions. All kMC simulations are performed at temperatures lower than 300 K. At such temperatures, an intermixing of deposited Co with substrate Cu atoms does not occur, as it will be discussed below.

Two different kinds of close-packed steps can be distinguished on a fcc(111) surface: the {100}-microfaceted step (A step) and the {111}-microfaceted step (B step). We consider atomistic processes near and on Co nanoislands along both A and B step edges.

Calculations of atomic relaxations and diffusion barriers are carried out using the MS method. The interatomic potentials for the system of Cu and Co atoms (Cu-Cu, Cu-Co, and Co-Co) are formulated in the second moment approximation of the tight-binding approach.¹⁷ The Korringa-Kohn-Rostocker Green's function method¹⁸ is used to create an *ab initio* data pool for the fitting of parameters of these potentials. Such potentials¹⁹ reproduce the bulk properties of Cu and Co crystals and the *ab initio* calculated properties of supported and embedded Co clusters. The details of the fitting procedure are described in Ref. 20. Previous studies^{21–23} have demonstrated that the combination of *ab initio* and tight-binding methods allows one to construct many-body potentials for low-dimensional systems providing a good approximation for atomic displacements found in *ab initio* calculations. The MS simulations are performed with a finite slab of nine layers arranged according to the ABC-fcc sequence of (111) fcc surfaces. Each layer contains 1400 atoms. Two bottom layers are kept fixed and periodic boundary conditions are applied in the surface plane.

Our experiments were performed in an ultrahigh vacuum system equipped with STM operating at low temperatures (6 K). Co was evaporated with a rate of ~ 0.1 ML/min onto a single crystal Cu(111) surface at various temperatures (130–300 K). Immediately after evaporation, the sample was transferred to the STM, where it was rapidly cooled to 6 K. This ensures that dynamical effects, due to the mobility of Co, are frozen out and the sample with the grown islands remains as prepared during investigation.

It is believed that intermixing of Co and Cu plays a significant role during epitaxial growth at RT.^{24–26} Molecular

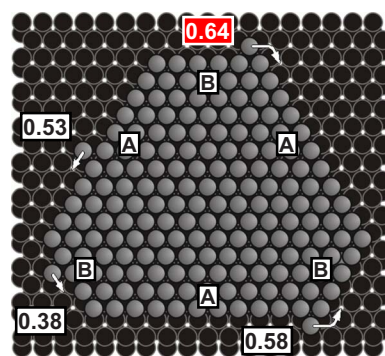


FIG. 1. (Color online) Anisotropic corner diffusion is the origin of the growth of triangular Co islands with A step edges. The barriers for operative (suppressed) atomic transitions are demonstrated using white (red/gray) rectangles. Black balls represent Cu atoms; dark gray balls correspond to Co atoms.

dynamics—Monte Carlo simulations of Gómez *et al.*^{24,25} at 540 K have indicated that intermixing between Co and Cu can occur through the ballistic induced alloying mechanism. Recent studies of Bozzolo *et al.*²⁶ by means of Bozzolo-Ferrante-Smith method for alloys revealed that incorporation of Co atoms into the surface takes place at $T \geq 300$ K. Usually, the intermixing of Co and Cu is associated with the formation of vacancy islands in the Cu substrate. In our experiments, we do not observe any vacancies at temperatures below 300 K, whereas at 310 K and higher, we do observe vacancy islands. At 345 K, the vacancy island density is strongly increased and, furthermore, we can directly observe rough islands likely to be due to alloying of Co and Cu. To explain the growth at RT and below, we can, therefore, safely exclude intermixing in our simulations.

III. RESULTS AND DISCUSSIONS

In this section, we reveal main atomistic processes responsible for the formation of triangular bilayer Co islands at RT. The kMC simulations of the growth of Co nanoislands at RT are presented and compared with the experimental measurements. We demonstrate the effect of the temperature on the growth regime. Finally, we reveal the effect of strain relaxations induced in the substrate and growing structures on the formation of nanoislands at RT.

A. Main atomistic events: Molecular static calculations

Deposited Co atoms randomly diffuse on the surface with a barrier of 0.04 eV and coalescence into islands. Several studies revealed that anisotropic corner diffusion of deposited atoms near small islands can significantly influence growth processes and can lead to the formation of compact triangular islands.^{15,27} First, we demonstrate that the growth of Co islands on Cu(111) in the early stages is also caused by anisotropic corner diffusion.

We consider a 1 ML high small Co island with both A and B steps (Fig. 1). When the Co atom approaches the corner of the island along an A step, it can either diffuse backward along the same step with the barrier of 0.53 eV or it can

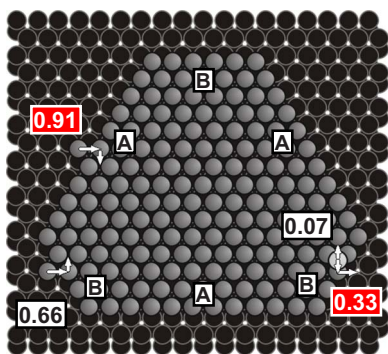


FIG. 2. (Color online) Interlayer mass transport between the first and the second Co layer is operative at B step. The barriers for operative (suppressed) atomic transitions are demonstrated using white (red/gray) rectangles. The ascended Co atom most likely exhibits the diffusion on top of the 1 ML Co island. Black balls represent Cu atoms; dark and light gray balls correspond to Co atoms.

make a corner hop toward a B step with the barrier of 0.58 eV. One can estimate the relative probability of the rate of the second event with respect to the rate of the first one using the formula $\nu_1/\nu_2 = \exp[(E_2 - E_1)/(k_B T)]$. The energy difference between two barriers is rather small (0.05 eV), and at RT we obtain that $\nu_1/\nu_2 = 0.15$. This implies that the corner diffusion of Co atoms from an A to a B step takes place at RT. In contrast, a corner diffusion at a B step is strongly anisotropic: the diffusion barrier for the jump toward an A step is 0.64 eV, while a diffusion barrier along a B step is 0.38 eV. Thus, the relative probability of the rate of the corner diffusion at a B step with respect to the rate of the step-edge diffusion along a B step is 10^{-5} , i.e., almost zero. Therefore, the corner diffusion from a B to an A step is not operative at RT. These results suggest that triangular shaped Co nanoislands with an A step edges should be formed during early stages of the growth process.

However, the growth scenario is much more complicated due to the interlayer mass transport (IMT). Our calculations reveal that Co adatoms can exhibit the upward mass transport to the second layer through the exchange mechanism at step edges. Figure 2 depicts the atomic exchange processes responsible for the upward mass transport of Co atoms from the first to the second layer in the early stages of growth. The exchange barrier at a B step (0.66 eV) is found to be considerably smaller than the barrier at an A step (0.91 eV). The downward mass transport via atomic exchange occurs with barriers of 0.61 and 0.33 eV for an A and a B step, respectively.²⁸ We note that the barrier for the upward mass transport at an A step is too high and this process is suppressed at RT.²⁹ To understand the difference between atomic exchanges at A and B steps, we recall recent studies on mesoscopic relaxations at step edges.^{21,30} It was shown that the stress relief due to strain relaxations is larger for an A step. In other words, the average bond length in the vicinity of a B step is increased compared to an A step. According to Yu and Scheffler,³¹ a decreasing (increasing) corrugation of the potential increases (decreases) the barrier for exchange.

Once the Co adatom is on top of a 1 ML high Co island, it may exhibit the downward exchange at the step edge or the

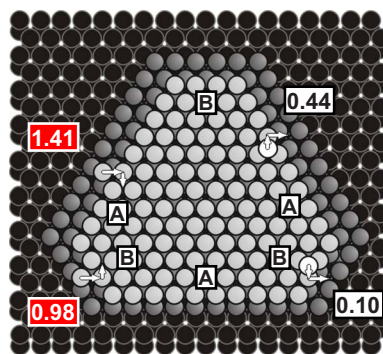


FIG. 3. (Color online) Interlayer mass transport between the second and the third layer of Co islands. The barriers for operative (suppressed) atomic transitions are demonstrated using white (red/gray) rectangles. Black balls represent Cu atoms; dark gray balls correspond to Co atoms of the first layer of Co cluster, light gray to of the second one, and white to of the third one.

hopping diffusion on top of the island. Our results presented in Fig. 2 demonstrate that the barrier for the hopping on top of the island is significantly smaller (about 0.07 eV) than the barrier to descent from top of the island via the exchange at the edge (0.33 eV). Therefore, the relative probability of the rate of the second event with respect to the rate of the first one $\nu_1/\nu_2 = \exp[(E_2 - E_1)/(k_B T)] = 10^{-5}$, i.e., almost zero. Thus, Co atoms can appear on top of a 1 ML high Co island due to the upward mass transport. A pair of Co atoms aggregated on top of 1 ML high islands forms a dimer, which does not dissociate at RT, because of a binding energy of 1.5 eV. A Co dimer can be considered as a nucleation center for growth of the second layer of the Co island. The subsequently deposited Co atoms diffuse on Cu(111), join the Co island, ascend on top of the first Co layer (Fig. 2), and increase the size of the second Co layer. The geometry of the second layer is unambiguously determined by the geometry of the underlying substrate. The natural limit of the growth of the second layer is set by the size of the first Co layer.

Now, we consider the main atomistic processes on 2 ML high Co islands (Fig. 3). Co atom can land on top of the 2 ML high island during deposition. Such Co atom diffusing on top of the second layer of the Co island (with barrier of 0.07 eV) can leave the top of the island via the exchange at an A (B) step edge with a barrier of 0.44 (0.10) eV. These events are operative; therefore, there is the IMT of Co atoms from the third to the second Co layer. On the contrary, there is no IMT of Co atoms from the second to the third layer because the barriers for the upward mass transport via the exchange processes are very large for both steps (1.41 eV for an A step and 0.98 eV for a B step). These results indicate that Co atoms tend to cover all possible sites on the second layer forming Co islands of a bilayer height.

To conclude this section, we would like to note that the diffusion barrier of a single Co adatom on a Cu(111) surface found within our MS calculations (0.04 eV) is in a very good agreement with the experimental result of Stroschio and Celotta³² (less than 0.05 eV). However, the same activation barrier reported by Prieto *et al.*,¹³ who used nucleation theory to fit the data, is considerably larger (0.19 eV). We

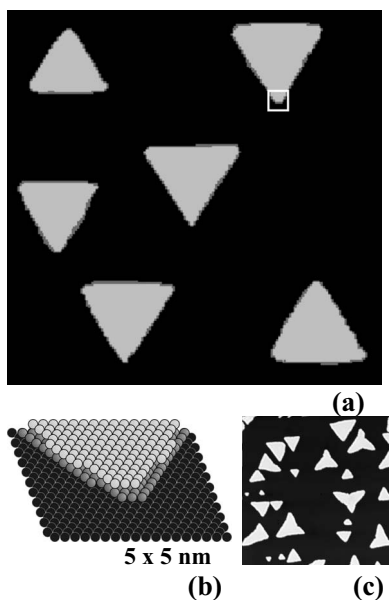


FIG. 4. (a) The morphology of Cu(111) surface exposed by 0.4 ML of Co atoms at 290 K: the kMC simulation. (b) The atomic resolution of the area marked on (a) with the white square. (c) The experimentally observed morphology. The area $100 \times 100 \text{ nm}^2$ is demonstrated in (a) and (c).

believe that the origin of this strong difference between the reported values is a number of assumptions lying in the basis of the phenomenological model exploited in Ref. 13. At the same time, the activation barrier for the step-edge diffusion (0.35 eV) determined by Prieto *et al.*¹³ is in agreement with our values (0.53 eV for step *A* and 0.38 eV for step *B*, Fig. 1). Additionally, the activation barrier for the diffusion of a single Co adatom on top of Co island found in our calculations (0.07 eV) fits also well to that reported in Ref. 13 (0.08 eV).

B. Kinetic Monte Carlo simulations and experimental results

Having discussed atomistic processes, we now turn to the kMC simulations of the self-assembly of Co nanoislands on Cu(111) at different temperatures. We shall demonstrate the key role played by specific atomistic events. As already pointed out, the anisotropic corner diffusion and the IMT between different layers should determine the structure of growing islands. In Fig. 4, we present the kMC simulations and the experimental results obtained at RT. They both demonstrate the formation of bilayer Co islands bounded by *A* steps. We revealed that the formation of the second Co layer via the IMT proceeds simultaneously with the growth of the first Co layer. Triangle islands with two possible orientations are observed. It corresponds to the different stacking faults of the first Co layer (fcc or hcp stacking). Within our simulations, we found that the relative amount of triangles with fcc stacking is 0.65 vs 0.35 with the hcp one. This observation fits well to the experimental data.

Note that the calculated islands are perfect triangles, though some of the experimental ones are slightly concave (mostly the larger islands). We explain this fact by the slight

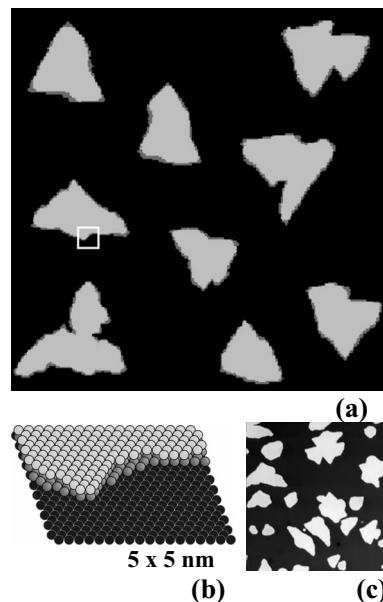


FIG. 5. (a) The morphology of Cu(111) surface exposed by 0.4 ML of Co atoms at 250 K: the kMC simulation. (b) The atomic resolution of the area marked on (a) with the white square. (c) The experimentally observed morphology. The area $100 \times 100 \text{ nm}^2$ is demonstrated in (a) and (c).

mismatch between the calculated and the experimental diffusion barriers (barriers in the calculations are underestimated). Thereby, the diffusivity in the experiment is too low to result in perfect triangles. However, already a very small change in barriers could lead to this. In order to check this, one has either to make measurements at a slightly higher temperature (this is difficult since there is intermixing) or to perform simulations at a slightly lower temperature. Indeed, our kMC simulations for 275 K demonstrate that concave triangles are formed, which is indicated on the small error in the determination of the barriers.

With increasing the coverage (up to 2.0 ML), Co islands can grow in the 3 ML high regime.¹³ To explain such behavior, we note that Co atoms may land on top of the 2 ML high island during the deposition. When two Co atoms diffusing on the island meet each other, the formation of Co dimer takes place. The probability of Co dimer formation increases with increasing the size of the island. Co dimers do not dissociate at RT since the binding energy of such dimers exceeds 1.0 eV.²⁹ Thus, the growth of the third layer takes place.

Decreasing the temperature from 290 to 250 K significantly affects the growth process of Co nanoislands. The results of our calculations and the STM image are shown in Fig. 5. One can see that Co islands are still 2 ML high but exhibit irregular shape. At 250 K, the corner mass transport of Co atoms from an *A* to a *B* step (Fig. 1) is hindered, leading to the growth of irregular islands.¹⁵

Upon further decreasing the temperature, the probability of the IMT between layers is reduced, and the two-dimensional growth mode is substituted by the three-dimensional one. For example, our results for 135 K presented in the Fig. 6 demonstrate that the growth mode is

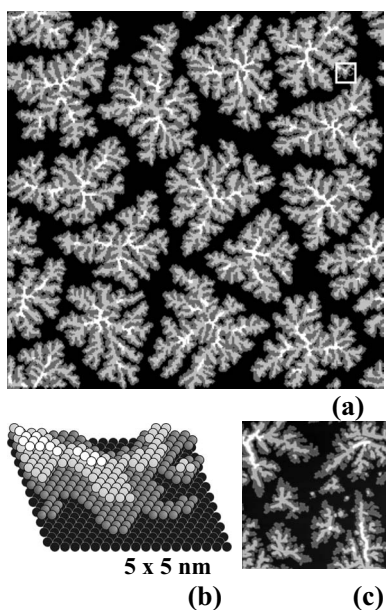


FIG. 6. (a) The morphology of Cu(111) surface exposed by 0.8 ML of Co atoms at 135 K: the kMC simulation. (b) The atomic resolution of the area marked on (a) with the white square. (c) The experimentally observed morphology. The area $100 \times 100 \text{ nm}^2$ is demonstrated in (a) and (c).

dramatically changed. The rate of the upward mass transport from the first to the second layer (Fig. 2) decreases; therefore, the first layer of the Co islands is not completely covered by the second layer. The IMT from the third layer to the second layer is not operative anymore, and 3 ML high Co islands grow under such conditions. Islands have a dendritic form because the step-edge diffusion (Fig. 1) is inhibited.

C. Effect of strain relaxations on the growth of nanoislands at room temperature

In this section, we demonstrate how atomic relaxations induced in the Cu substrate and in the Co nanoislands affect the growth process at RT. Previous studies showed that near steps and cluster edges, strain relaxations could be very strong. For instance, even in the homogenous systems, such as Cu/Cu(111), the strain induced by steps shifts the energy balance between fcc and hcp sites on vicinal Cu(111).³³ Strain affects the shape of a substrate and nanoislands during homo- and heteroepitaxy on Cu(111).²¹ It results in the change of details of atomic motion near the ascending³⁴ and descending³⁵ edges of the nanoislands. Strain in Cu(001) substrate influences the energy barriers for atomic exchange around embedded Fe islands and induces collective atomic transitions.³⁶ Strain is suspected to be the origin of the fast diffusion of small Co clusters on Cu(001).³⁷ Also, strain-induced change in the electronic structure of Cu(001) covered by nitrogen atoms was discovered recently.^{38,39}

To reveal the effect of atomic relaxations on the growth process of Co islands, we performed the following “gedanken experiment.” We excluded strain induced in the Cu substrate and in Co nanoislands and calculated the diffusion barriers for all atomic events discussed above. We revealed that

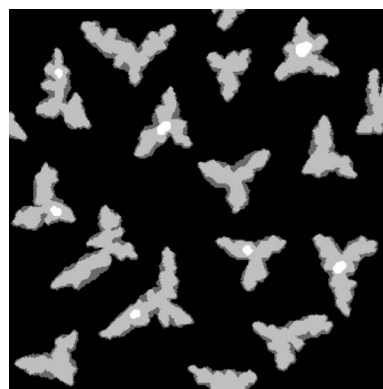


FIG. 7. The morphology of Cu(111) surface exposed by 0.4 ML of Co atoms at 290 K: the kMC simulation. Strain relaxations are excluded. The area $100 \times 100 \text{ nm}^2$ is demonstrated.

the values of barriers for the certain number of atomic events are changed dramatically. For instance, the barrier for the Co-monomer diffusion is strongly enhanced, 0.10 eV vs 0.04 eV for a fully relaxed system. Also, the corner mass transport of Co atoms from a *B* to an *A* step and in the opposite direction is inhibited. When Co atom approaches the corner of the island along an *A* step, it makes a corner hop toward a *B* step with the barrier of 0.74 eV (vs 0.58 eV for a fully relaxed geometry, see Fig. 1). Also, the barrier for the corner diffusion from a *B* to an *A* step is suppressed because of the barrier of 0.82 eV (vs 0.64 eV for a fully relaxed geometry). Our calculations indicate that the rate of the IMT between different layers decreases as well. For instance, without strain, the barriers for the downward mass transport of Co from the third to the second layer via exchange have the following values: at an *A* step edge, 0.74 eV (vs 0.44 eV in a fully relaxed geometry, Fig. 3), and at a *B* step edge, 0.32 eV (vs 0.10 eV in a fully relaxed geometry, Fig. 3). As a result, the downward mass transport of Co atoms landing on top of the second Co layer is suppressed.

Figure 7 demonstrates the results of the kMC simulations of growth process at RT in the absence of strain relaxations. The formation of triangular bilayer Co nanoislands (compare with Fig. 4) does not take place. The inhibited corner mass transport and suppressed IMT lead to the formation of irregular islands of 1–3 ML high. These results indicate that strain relaxations play a significant role during epitaxial growth of thin Co films on Cu(111).

IV. CONCLUSIONS

In conclusion, we explained on the atomic scale the formation of triangular bilayer Co islands on Cu(111) at room temperature. We revealed that growth of 2 ML high islands takes place starting from the early deposition stages, and exchange processes at the edges of nanoislands are responsible for such growth scenario. Taking all relevant atomistic

processes into account, we performed detailed kMC simulations in the temperature range 130–300 K. We found a perfect agreement with the experimental observations showing the gradual transformation from compact triangular islands at room temperatures over compact irregular islands to dendritic shaped islands at low temperatures. It was demonstrated that the preference of forming bilayer high islands disappears at low temperatures. It was shown that strain re-

laxations play a significant role during the growth process of Co nanoislands on Cu(111).

ACKNOWLEDGMENTS

This work was supported by Deutsche Forschungsgemeinschaft (SPP1165, SPP1153).

- ¹H. Brune, Surf. Sci. Rep. **31**, 121 (1998); F. J. Himpsel, J. E. Ortega, G. J. Mankey, and R. F. Willis, Adv. Phys. **47**, 511 (1998).
- ²J. de la Figuera, J. E. Prieto, C. Ocal, and R. Miranda, Phys. Rev. B **47**, 13043 (1993).
- ³J. de la Figuera, J. E. Prieto, G. Kostka, S. Müller, C. Ocal, R. Miranda, and K. Heinz, Surf. Sci. **349**, L139 (1996).
- ⁴K. Heinz, S. Müller, and L. Hammer, J. Phys.: Condens. Matter **11**, 9437 (1999).
- ⁵M. Ø. Pedersen, A. Bönicke, E. Lægsgaard, I. Stensgaard, A. Ruban, J. K. Nørskov, and F. Besenbacher, Surf. Sci. **387**, 86 (1997).
- ⁶A. L. Vázquez de Parga, F. J. García-Vidal, and R. Miranda, Phys. Rev. Lett. **85**, 4365 (2000).
- ⁷L. Diekhöner, M. A. Schneider, A. N. Baranov, V. S. Stepanyuk, P. Bruno, and K. Kern, Phys. Rev. Lett. **90**, 236801 (2003).
- ⁸U. Alkemper, C. Carbone, E. Vescovo, W. Eberhardt, O. Rader, and W. Gudat, Phys. Rev. B **50**, 17496 (1994).
- ⁹G. J. Mankey, R. F. Willis, and F. J. Himpsel, Phys. Rev. B **47**, 190 (1993).
- ¹⁰J. Osterwalder, T. Greber, E. Wetli, J. Wider, and H. J. Neff, Prog. Surf. Sci. **64**, 65 (2000).
- ¹¹K. Morgenstern, J. Kibsgaard, J. V. Lauritsen, E. Lægsgaard, and F. Besenbacher, Surf. Sci. **601**, 1967 (2007).
- ¹²M. Wasniowska, N. Janke-Gilman, W. Wulfhekel, M. Przybylski, and J. Kirschner, Surf. Sci. **601**, 3073 (2007).
- ¹³J. E. Prieto, J. de la Figuera, and R. Miranda, Phys. Rev. B **62**, 2126 (2000).
- ¹⁴K. A. Fichthorn and W. H. Weinberg, J. Chem. Phys. **95**, 1090 (1991).
- ¹⁵S. Ovesson, A. Bogicevic, and B. I. Lundqvist, Phys. Rev. Lett. **83**, 2608 (1999).
- ¹⁶A. Bogicevic, J. Strömquist, and B. I. Lundqvist, Phys. Rev. Lett. **81**, 637 (1998); J. Jacobsen, B. H. Cooper, and J. P. Sethna, Phys. Rev. B **58**, 15847 (1998); J. M. Pomeroy, J. Jacobsen, C. C. Hill, B. H. Cooper, and J. P. Sethna, *ibid.* **66**, 235412 (2002); S. Ovesson, A. Bogicevic, G. Wahnström, and B. I. Lundqvist, *ibid.* **64**, 125423 (2001); K. A. Fichthorn and M. Scheffler, Phys. Rev. Lett. **84**, 5371 (2000); K. A. Fichthorn, M. L. Merrick, and M. Scheffler, Phys. Rev. B **68**, 041404(R) (2003); M. Müller, K. Albe, C. Busse, A. Thoma, and T. Michely, *ibid.* **71**, 075407 (2005).
- ¹⁷V. Rosato, B. Guillope, and B. Legrand, Philos. Mag. A **59**, 321 (1989); F. Cleri and V. Rosato, Phys. Rev. B **48**, 22 (1993).
- ¹⁸K. Wildberger, V. S. Stepanyuk, P. Lang, R. Zeller, and P. H. Dederichs, Phys. Rev. Lett. **75**, 509 (1995); V. S. Stepanyuk, W. Hergert, K. Wildberger, R. Zeller, and P. H. Dederichs, Phys. Rev. B **53**, 2121 (1996).
- ¹⁹The potentials are used in the form of Ref. 17. The parameters are the following: for Cu-Cu, $A^1=0.0$ eV, $A^0=0.0854$ eV, $\xi=1.2243$ eV, $p=10.939$, $q=2.2799$, $r_0=2.5563$ Å; for Co-Cu, $A^1=-1.5520$ eV, $A^0=-0.0372$ eV, $\xi=0.8522$ eV, $p=7.6226$, $q=5.5177$, $r_0=2.4995$ Å; for Co-Co, $A^1=0.0$ eV, $A^0=0.1209$ eV, $\xi=1.5789$ eV, $p=11.3914$, $q=2.3496$, $r_0=2.4953$ Å.
- ²⁰N. A. Levanov, V. S. Stepanyuk, W. Hergert, D. I. Bazhanov, P. H. Dederichs, A. Katsnelson, and C. Massobrio, Phys. Rev. B **61**, 2230 (2000).
- ²¹O. V. Lysenko, V. S. Stepanyuk, W. Hergert, and J. Kirschner, Phys. Rev. Lett. **89**, 126102 (2002); V. S. Stepanyuk, D. I. Bazhanov, A. N. Baranov, W. Hergert, P. H. Dederichs, and J. Kirschner, Phys. Rev. B **62**, 15398 (2000).
- ²²V. S. Stepanyuk, A. N. Baranov, D. V. Tsviln, W. Hergert, P. Bruno, N. Knorr, M. A. Schneider, and K. Kern, Phys. Rev. B **68**, 205410 (2003).
- ²³V. S. Stepanyuk, A. L. Klavskyuk, W. Hergert, A. M. Saletsky, P. Bruno, and I. Mertig, Phys. Rev. B **70**, 195420 (2004); S. Pick, V. S. Stepanyuk, A. L. Klavskyuk, L. Niebergall, W. Hergert, J. Kirschner, and P. Bruno, *ibid.* **70**, 224419 (2004); R. A. Miron and K. A. Fichthorn, Phys. Rev. Lett. **93**, 128301 (2004); K. Sastry, D. D. Johnson, D. E. Goldberg, and P. Bellon, Phys. Rev. B **72**, 085438 (2005); V. S. Stepanyuk, A. L. Klavskyuk, L. Niebergall, A. M. Saletsky, W. Hergert, and P. Bruno, Phase Transitions **78**, 61 (2005).
- ²⁴L. Gómez, C. Slutzky, J. Ferrón, J. de la Figuera, J. Camarero, A. L. Vázquez de Parga, J. J. de Miguel, and R. Miranda, Phys. Rev. Lett. **84**, 4397 (2000).
- ²⁵L. Gómez, C. Slutzky, and J. Ferrón, Phys. Rev. B **71**, 233402 (2005).
- ²⁶G. Bozzolo, D. Farías, A. L. Vázquez de Parga, and R. Miranda, Surf. Rev. Lett. **11**, 591 (2000).
- ²⁷H. Brune, H. Röder, K. Bromann, K. Kern, J. Jacobsen, P. Stolze, K. Jacobsen, and J. Nørskov, Surf. Sci. **349**, L115 (1996); J. Jacobsen, K. W. Jacobsen, and J. K. Nørskov, *ibid.* **359**, 37 (1996).
- ²⁸Similar processes can occur at kinks of Co nanoislands. However, our studies show that the main results of our work are not affected if atomistic processes at kinks are taken into account.
- ²⁹An atomistic process characterized by the diffusion barrier E_D can be either operative or suppressed depending on the experimental conditions (temperature and flux). The submonolayer deposition regime (with a characteristic coverage $D \sim 0.1$ ML) is examined within our study. Therefore, the characteristic time scale t_c of the growth process is $D/F \sim 10$ s. The activation time of the atomistic process can be estimated using the expression

- $t_D \sim v_0^{-1} \exp(E_D/k_B T)$, where $v_0 = 10^{12}$ Hz and $k_B = 0.086$ meV/K. The considered event is operative only if $t_D < t_c$, otherwise it is suppressed. In other words, all atomistic processes having activation barriers $E_D > E_{cr} = 0.75$ eV are inhibited at RT and $F = 0.001$ ML/s. The magnitude of threshold value E_{cr} depends on the temperature T (E_{cr} decreases with decreasing of T).
- ³⁰O. V. Lysenko, V. S. Stepanyuk, W. Hergert, and J. Kirschner, Phys. Rev. B **68**, 033409 (2003).
- ³¹B. D. Yu and M. Scheffler, Phys. Rev. Lett. **77**, 1095 (1996).
- ³²J. A. Stroscio and R. J. Celotta, Science **306**, 242 (2004).
- ³³M. Giesen and H. Ibach, Surf. Sci. **529**, 135 (2003).
- ³⁴D. V. Tsivlin, V. S. Stepanyuk, W. Hergert, and J. Kirschner, Phys. Rev. B **68**, 205411 (2003).
- ³⁵V. S. Stepanyuk, D. I. Bazhanov, W. Hergert, and J. Kirschner, Phys. Rev. B **63**, 153406 (2001).
- ³⁶R. C. Longo, V. S. Stepanyuk, W. Hergert, A. Vega, L. J. Gallego, and J. Kirschner, Phys. Rev. B **69**, 073406 (2004).
- ³⁷R. A. Miron and K. A. Fichthorn, Phys. Rev. B **72**, 035415 (2005).
- ³⁸D. Sekiba, K. Nakatsuji, Y. Yoshimoto, and F. Komori, Phys. Rev. Lett. **94**, 016808 (2005).
- ³⁹D. Sekiba, Y. Yoshimoto, K. Nakatsuji, Y. Takagi, T. Iimori, S. Doi, and F. Komori, Phys. Rev. B **75**, 115404 (2007).